Measurement of the dead layer thickness in a p-type point contact germanium detector*

Hao Jiang(江灏)[1,2] Qian Yue(岳骞)[1,2;1)] Yu-Lan Li(李玉兰)[1,2;2)] Ke-Jun Kang(康克军)[1,2]
Yuan-Jing Li(李元景)[1,2] Jin Li(李金)[1,2] Shin-Ted Lin(林兴德)[3] Shu-Kui Liu(刘书魁)[1,2]
Hao Ma(马豪)[1,2] Jing-Lu Ma(马菁露)[1,2] Jian Su(苏健)[1,2] Henry Tsz-King Wong(王子敬)[4]
Li-Tao Yang(杨丽桃)[1,2] Wei Zhao(赵伟)[1,2] Zhi Zeng(曾志)[1,2]

[1] Dept. of Engineering Physics, Tsinghua University, Beijing 100084, China
[2] Key Laboratory of Particle & Radiation Imaging (Tsinghua University), Ministry of Education, Beijing 100084, China
[3] College of Physical Science and Technology, Sichuan University, Chengdu 610064, China
[4] Institute of Physics, Academia Sinica, Taipei 11529, China

Abstract: A 994 g mass p-type PCGe detector has been deployed during the first phase of the China Dark matter EXperiment, aiming at direct searches for light weakly interacting massive particles. Measuring the thickness of the dead layer of a p-type germanium detector is an issue of major importance since it determines the fiducial mass of the detector. This work reports a method using an uncollimated ^{133}Ba source to determine the dead layer thickness. The experimental design, data analysis and Monte Carlo simulation processes, as well as the statistical and systematic uncertainties are described. A dead layer thickness of 1.02 mm was obtained based on a comparison between the experimental data and the simulated results.

Keywords: dead layer, CDEX, PPCGe, Monte Carlo

PACS: 95.35.+d, 29.40.-n **DOI:** 10.1088/1674-1137/40/9/096001

1 Introduction

The China Dark matter EXperiment (CDEX) aims at direct searches for light Weakly Interacting Massive Particles (WIMPs), employing a point-contact germanium detector (PCGe) at the China Jinping Underground Laboratory (CJPL), which has about 2400 m of rock overburden. A previous paper reports the results from the CDEX phase I experiment (CDEX-1) using a p-type PCGe (PPCGe) detector (CDEX-1A) of mass 994 g [1]. PPCGe detectors have excellent properties for dark matter search experiments. A small area of the point contact electrode, which can significantly reduce the capacitance, results in low electronic noise and energy threshold [2]. The CDEX-1A detector can reach a threshold of ∼400 eVee ("ee" denotes electron-equivalent energy) [3]. Besides that, the localized weighting potential resulting in distinct current pulses from individual interaction charge clouds provides the ability to distinguish between Single Site Events (SSE) and Multiple Site Events (MSE), which can be used to discriminate the signals from the background [4].

However, PPCGe detectors have a dead layer at the surface caused by lithium diffusion. Events generated in the dead layer will lead to a slow rise time pulse and an incomplete charge collection because of the very weak electric field in this region [5–7]. Burns et al. found that the dead layer was composed of two layers: an inactive layer where no charge can be collected by the electrodes, and a transition layer where the charge collection efficiency increases from zero to one [8]. As a result, the events in the dead layer cannot provide the primary energies that are deposited in the detector and should be discriminated from the bulk events by applying an efficiency correction. At the same time, the fiducial volume and mass should also be calculated based on the thickness of the dead layer.

The characteristics of the dead layer have been investigated in the literature. In 1998, Clouvas used an empirical formula to describe the charge collection in the dead layer. The authors found a good agreement between the simulated spectrum and the experimental spectrum based on this formula. However, they got a dead layer thickness of 2.5 mm, which disagreed hugely

Received 21 March 2016
∗ Supported by National Natural Science Foundation of China (10935005, 10945002, 11275107, 11175099)
1) E-mail: yueq@mail.tsinghua.edu.cn
2) E-mail: yulanli@mail.tsinghua.edu.cn

with the manufacturer's result of 0.5 mm [9]. N. Q. Huy et al. showed that the dead layer thickness increases over time because lithium diffusion is happening all the time [10]. Thus, it is not reliable to use the dead layer thickness given by the manufacturer. Since the systematic uncertainty contribution from the fiducial mass of the CDEX-1A detector should be evaluated in CDEX-1A data analysis, it is essential to accurately measure the thickness and uncertainty of the dead layer.

This article reports a measurement of the dead layer thickness of the PPCGe detector from the CDEX-1A experiment with an uncollimated ^{133}Ba source. In the following sections, the experimental design, data analysis and Monte Carlo simulation processes, as well as the statistical and systematic uncertainties are discussed.

2 Detector geometry

The CDEX-1A detector was fabricated by Canberra Company in 2010 with a dead layer thickness of 0.5 mm given by the manufacturer. The germanium crystal has a diameter of 62.2±0.1 mm and a height of 62.3±0.1 mm and is encapsulated in a Oxygen Free High Conductivity (OFHC) copper cryostat. The copper thickness at the endcap side opposite to the point contact is 1.5±0.1 mm and at the side is 2.0±0.1 mm. The distance between the endcap and the germanium crystal is 4.5±0.1 mm and there is no other material but vacuum between them. At the side, there are some supports, foils and screws made of OFHC copper, lead and brass. The point contact is at the bottom of the crystal and connected to a brass pin to read out the signals. The geometry of the CDEX-1A detector is shown in Fig. 1.

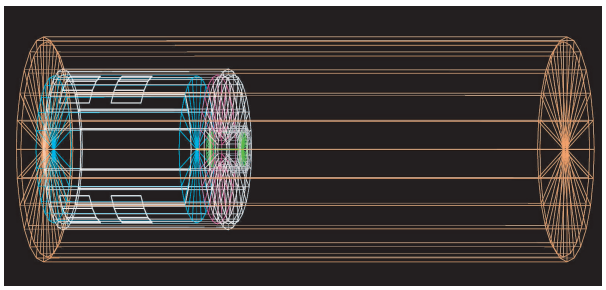

Fig. 1. (color online) The structure of the CDEX-1A detector.

The PPCGe detector can be distinguished into two parts: the dead layer, where no charge or only part of the charge is collected by the electrodes, and a bulk part, in which all charge produced is fully collected by the electrodes. Signals generated in the dead layer have a much slower rise time and an incomplete charge collection, as shown in Fig. 2.

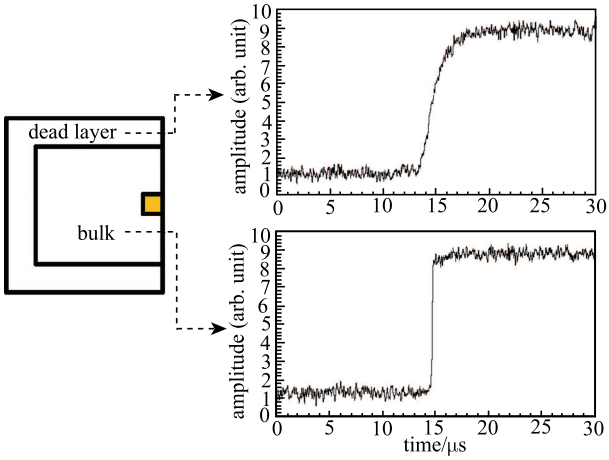

Fig. 2. (color online) Typical signals at ∼10 keV from dead layer (top) and bulk (bottom). Signals from the dead layer have a much slower rise time and an incomplete charge collection, e.g. the actual deposited energy is larger than 10 keV. The size of the point and the thickness of the dead layer are not shown to scale.

3 Experimental process

A ^{133}Ba source is an excellent source to measure the dead layer because it has several photoelectron peaks from low to high energy as shown in Table 1. Lower energy photons are more likely to interact in the dead layer compared to higher energy photons. Therefore, the 81 keV photoelectron peak of the ^{133}Ba source is mainly used to study the dead layer thickness. Due to the incomplete charge collection, the surface events do not contribute to the photoelectron peaks at all. As a consequence, the thickness of the dead layer will affect the detection efficiency of photoelectron peaks between gamma rays of different energies. As the precise activity of the ^{133}Ba source is unknown, the dead layer thickness can be derived by comparing a higher energy photoelectron peak of the ^{133}Ba source to the 81 keV photoelectron peak.

Table 1. Gamma ray energies and intensities of a ^{133}Ba source [11].

energy/keV	intensity (%)
53.16	2.14
79.61	2.65
81.00	32.95
160.61	0.64
223.24	0.45
276.40	7.16
302.85	18.34
356.01	62.05
383.85	8.94

The steps to measure the dead layer thickness are as follows. First, as what we need to measure is the average thickness of the dead layer, an uncollimated ^{133}Ba source was used to get the ratios of different photoelectron peaks in experiment. Secondly, as all the parameters were known apart from the dead layer thickness, including the detector geometries, shielding geometries and source position, a series of dead layer thicknesses were assumed to get the simulated results of the ratios, respectively. At last, the dead layer thickness was derived by comparing the experimental data and the simulation data. This method has also been used by the GERDA and MAJORANA Collaborations to get the dead layer thickness of their germanium detectors [12].

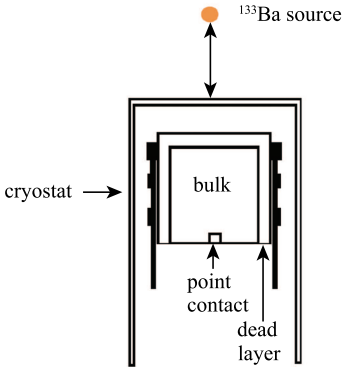

Fig. 3. (color online) The layout of the CDEX-1A PPCGe detector and source position. The dimensions of the point contact and dead layer are not shown to scale.

The crystal of this detector was fabricated with a side-hold structure made of OHFC and other material of which the depth is not uniform, as shown in Fig. 3. This makes the measurement of dead layer in the lateral surface quite difficult. So we just measure the dead layer of the top surface of the detector. In our experiment, an uncollimated ^{133}Ba source was put right above the detector endcap, as shown in Fig. 3. A height gauge was used to fix the ^{133}Ba source and measure the distance between the source and the endcap. Signals from the point contact electrode were fed into a pulsed reset preamplifier. Then, a shaping amplifier at 6 μs shaping time and a 14 bit 100 MHz flash analog-to-digital convertor (FADC) were used to shape, amplify and digitize the signals.

4 Results and discussion

4.1 Experimental data analysis

Because of the special work pattern of the preamplifier used with the CDEX-1A PPCGe detector, the detection efficiency of the preamplifier is energy-dependent, which can affect the photoelectron peak ratios between gamma rays of different energies. What is more, the accidental coincidence events can also change the photoelectron peak ratios. As the experiment is based on the comparison between experimental and simulated results, it is necessary to assure that the experimental conditions coincide with the simulated ones. In order to achieve this goal, several events selections and rejections should be done in the experimental data before we can get the correct experimental spectrum of a ^{133}Ba source.

4.1.1 Event selection from preamplifier reset period

A pulsed reset preamplifier is used with the CDEX-1A PPCGe detector to achieve ultra-low noise level. The charge and discharge processes are shown in Fig. 4(a). The baseline level of the preamplifier decreases with time due to the continuous leakage current of the detector itself and the induced current (signal 1) from the incident particles. This is the so called charge process. When the baseline level reaches the reset point, the preamplifier is reset immediately to make it work again. This is the so called discharge process.

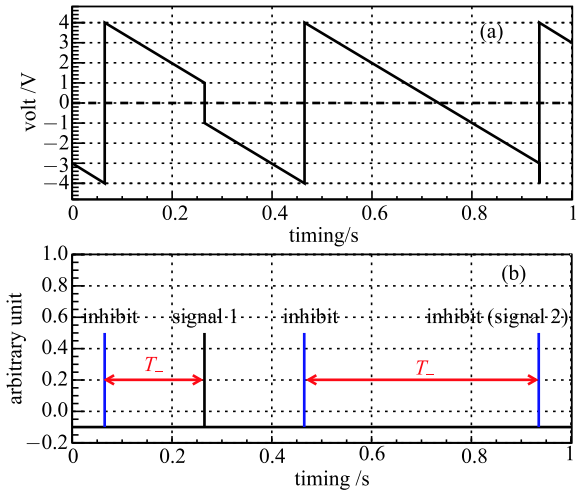

Fig. 4. (color online) (a) Baseline level of the preamplifier. (b) Each time the preamplifier is reset, a reset inhibit signal is obtained. T_- is the time between the event (indicated with "signal 1" in the figure) and its nearest preceding reset inhibit signal. The detector is reset immediately by a large induced current from an incident particle (indicated with "signal 2" in the figure) and the "signal 2" will give incomplete energy information for that incident large energy event. So we choose a small T_- range in order to get rid of this kind of event.

Each time the preamplifier is reset, a reset inhibit signal is obtained as shown in Fig. 4(b). The typical average reset period is about 0.4 s with a ^{133}Ba source located at the distance of 73 mm for the CDEX-1A PPCGe detector. T_- is the time difference between the event and its nearest prior reset inhibit signal.

If the electronic level difference between the baseline level to the reset point is less than the voltage drop produced by a large induced current from an incident particle, the output signal just represents part of the total energy deposited in the detector, such as signal 2 shown in Fig. 4(b). This effect decreases the detection efficiency for the events from low to high energies. Higher energy particles reset the preamplifier more easily. That means the detection efficiency is energy-dependent, which will change the ratios of different photoelectron peaks.

The event selection from the preamplifier reset period was derived from the parameter T_- distribution, aiming at choosing a region where the detection efficiency was energy-independent to make sure that the ratios of different photoelectron peaks were not affected. Figure 5 shows the relationship between the event counts of a ^{133}Ba source and T_- at the source position of 73 mm. It is shown that the event counts dropped rapidly at T_- > 0.22 s, which meant some gamma rays were lost as the preamplifier was reset by them. In order to avoid the efficiency problem, we set T_- cut at 0.2 s to reject the events with $T_- > 0.2$ s.

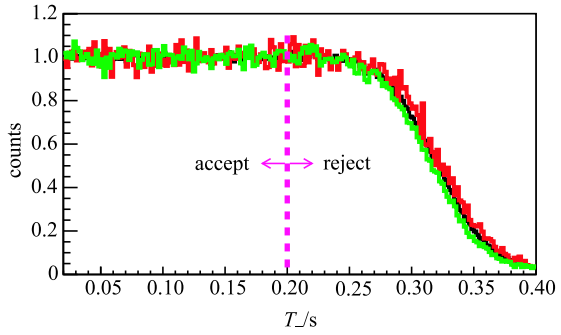

Fig. 5. (color online) Relationship between event counts and T_- at source position 73 mm. The black line represents the event counts of the total spectrum. The red line represents the event counts of the 81 keV photoelectron peak. The green line represents the event counts of the 356 keV photoelectron peak. The counts for photoelectron peaks of the 81 keV, 356 keV and the total spectrum have been normalized to the same scale in this figure.

4.1.2 Accidental coincidence event rejection

As the time window of our DAQ system is 80 μs, there are some accidental coincidence events in the time window. Since the pulse amplitude was used to do the energy calibration, some lower energy events could be masked by higher energy events in the same time window, which would also change the ratios of different energy peaks. For example, while a 81 keV photon and a 356 keV photon are both detected by the detector within 80 μs, we will consider the signal as a 356 keV photon. The 81 keV photon is lost. Accidental coincidence events can decrease the event rates of low energy photons and change the photoelectron peak ratios between gamma rays of different energies. However, this effect is not considered in the simulation. The rejection criterion of accidental coincidence events is based on the correlation between the maximal amplitude (Amp) and the integral of the signal pulse (Q).

Figure 6 shows the relationship between Q and Amp. If there is only one event in the time window which is the normal event, the integral of the signal pulse (Q) is in direct proportion to the maximal amplitude (Amp). As Fig. 6 shows, the main distribution band is normal events because the Q-Amp distribution has a linear correlation. While there are two or more accidental coincidence events in the time window, the integral of the signal pulse (Q) is bigger or smaller than the normal signal with the same maximal amplitude. The signal selection region is defined at 3σ of the linear events distribution band [13].

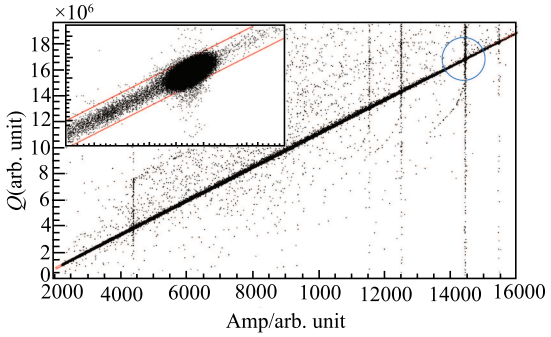

Fig. 6. (color online) All the events outside the two red lines are rejected. The inset figure shows the 356 keV photoelectron peak and the 3σ cut lines.

The relationship between the real rate and the measured rate of one specific energy photoelectron peak is given by the following formula [14]:

$$R_m = R_r - 2\tau R_r R_{\rm tot} = R_r(1-2\tau R_{\rm tot}), \quad (1)$$

where R_m refers to the measured rate of the specific energy photoelectron peak after the accidental coincidence events rejection, R_r refers to the real rate of the specific energy photoelectron peak detected by the detector, τ refers to the time window of the accidental coincidence, and $R_{\rm tot}$ refers to the real event rate of the whole spectrum detected by the detector.

What we want to know is the R_r, which cannot be obtained due to the accidental coincidence effect, and what we get after doing the accidental coincidence event rejection is R_m. As the parameter $1-2\tau R_{\rm tot}$ in formula (1) is a constant term which is energy-independent, it will not change the value of ratios of different photoelectron peaks. That means the ratios of measured rates

after accidental coincidence events rejection are equal to the ratios of real rates. After using the accidental coincidence events rejection, the measured rates were used to derive the ratios of different photoelectron peaks without any correction.

4.1.3 Experimental results

Figure 7 shows an experimental spectrum of a ^{133}Ba source obtained after applying all the selections and rejections. The distance between the source and the endcap is 73 mm which is a good compromise between efficiency and not having too many coincidences. In this spectrum, there were five explicit photoelectron peaks which were used to obtain the dead layer thickness: 81 keV, 276 keV, 303 keV, 356 keV and 384 keV. The 161 keV and 223 keV photoelectron peaks of the ^{133}Ba source were not used because they were significantly smaller than the other five peaks.

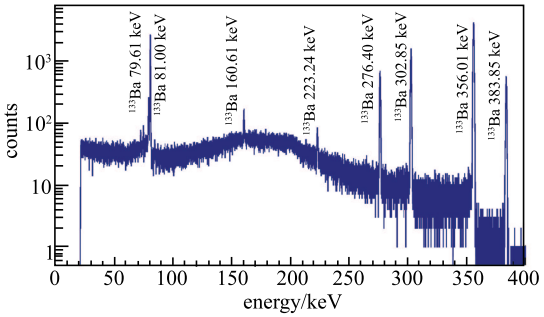

Fig. 7. (color online) An experimental spectrum of the ^{133}Ba source from the CDEX-1A PPCGe detector

The fitting result of the 81 keV photoelectron peak is shown in Fig. 8(a). As the photoelectron peaks of the 79.61 keV and the 81 keV are too close to each other, two Gaussian functions and a linear function are applied to fit the two peaks and the background. The green line represents the Gaussian function of the 79.61 keV photoelectron peak, the blue line represents the Gaussian function of the 81 keV photoelectron peak, the black line represents the linear function of the background and the red line represents the combined results.

The fitting result of the 356 keV photoelectron peak is shown in Fig. 8(b). A Gaussian function and linear function are used to describe the peak region.

The peak area can be calculated using the formula below:

$$A = \sqrt{2\pi}\sigma H/W, \tag{2}$$

where A refers to the peak area of the photoelectron peak, σ refers to the σ of the fitting result of a Gaussian function, H refers to the peak height and W refers to the width of the energy bins.

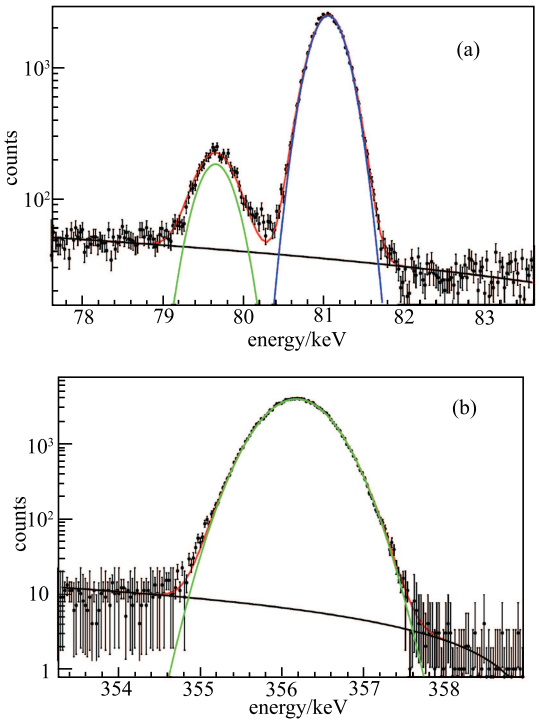

Fig. 8. (color online) The fitting results of the ^{133}Ba source. (a) The fitting result of the 79.6 keV and the 81 keV photoelectron peaks. (b) The fitting result of the 356 keV photoelectron peak.

Using the parameters derived from the fitting result of Fig. 8, the ratios of different photoelectron peaks were obtained as below:

$$R(81\text{ keV}, 356\text{ keV}) = \frac{A(356\text{ keV})}{A(81\text{ keV})} = \frac{H_{356\text{ keV}}\sigma_{356\text{ keV}}}{H_{81\text{ keV}}\sigma_{81\text{ keV}}}.$$

As the dead layer is at the surface of the germanium detector, lower energy photons are more sensitive to it than higher energy photons. The denominator of the ratio was fixed with the 81 keV peak area and the numerator was changed from the 276 keV peak area to the 384 keV peak area. Other experimental results were obtained by the same method and shown in Table 2. The results were also normalized by the branching ratios (BR) of the ^{133}Ba source. The energy peak ratios decrease with increasing energy.

Table 2. Different energy peak ratios before and after BR normalization with a distance of 73 mm between the source to the detector endcap.

energy peak	energy peak ratio with 81 keV(before BR normalization)	energy peak ratio with 81 keV(after BR normalization)
276 keV	0.393±0.005	1.809
303 keV	0.953±0.009	1.712
356 keV	2.853±0.023	1.515
384 keV	0.390±0.005	1.437

4.2 Simulation data analysis

Geant4 9.5 [15, 16] was used to simulate the initial interaction of a ^{133}Ba source in the PPCGe detector in the CDEX-1A experiment and to construct all the structures of the CDEX-1A detector and shieldings into the simulation program as shown in Fig. 1. A code was developed to consider the cascade effect of the ^{133}Ba nucleus [17]. In the simulation, the dead layer thickness was scanned from 0 mm to 1.4 mm to get different simulated results of the ^{133}Ba source. A simulated spectrum of ^{133}Ba source is shown in Fig. 9. Since the spectrum of the surface events with continuous energy distribution cannot influence the ratios of different photoelectron peaks, only the bulk events were considered in the simulation, while the surface events were not included. Compared with the simulated spectrum in Fig. 9, some photoelectron peaks with low statistics are not distinct and are submerged in the background in the experimental spectrum in Fig. 7, whose contribution is mainly from the surface events.

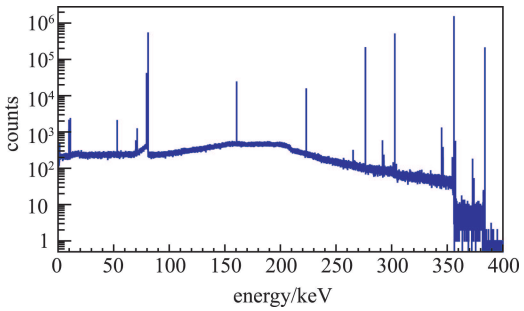

Fig. 9. (color online) The simulated spectrum of the ^{133}Ba source. The distance between the source and the endcap is 73 mm, and the dead layer thickness is assumed to be 1.0 mm. The energy resolution of the detector is not considered in the simulation.

As depicted in Fig. 10, the points for different dead layer thicknesses with statistical error bars from the simulation show the ratio of the number of events in the 81 keV photoelectron peak to that in the 356 keV photoelectron peak. A quadratic fitting function provides a good description to the simulation data. The horizontal band with 1σ error bar shows the ratio that was measured in the experimental data and the vertical band with 1σ error bar determines the thickness of the dead layer by comparing the experimental ratio and the simulation data implementing the interpolation method. Using this method, a series of results were obtained as shown in Table 3.

4.3 Statistical and systematic uncertainties

4.3.1 Statistical uncertainty

In Table 3, several results for the dead layer thickness were obtained by choosing different photoelectron peaks of the ^{133}Ba source. As the peak areas were achieved by the formula (2), the statistical uncertainties of these results can be achieved by the following steps.

Step 1: Using the formula below to get the statistical uncertainties of different photoelectron peak ratios:

$$\sigma_R = \sigma\left(\frac{A_1}{A_2}\right) = \frac{H_1}{H_2}\frac{\sigma_1}{\sigma_2}\sqrt{\frac{\sigma_{H_1}^2}{H_1^2}+\frac{\sigma_{\sigma_1}^2}{\sigma_1^2}+\frac{\sigma_{H_2}^2}{H_2^2}+\frac{\sigma_{\sigma_2}^2}{\sigma_2^2}}, \quad (3)$$

where σ_R refers to the statistical uncertainties of peak ratios, A_i refers to the peak area of photoelectron peak i, H_i refers to the peak height of photoelectron peak i, and σ_i refers to the sigma of photoelectron peak i $(i=1,2)$. All the uncertainties of peak ratios are also shown in Table 2.

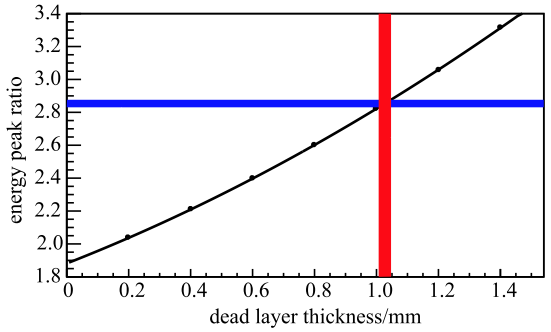

Fig. 10. (color online) Determination of the thickness of the dead layer at the source position of 73 mm. The black points are from the simulation, providing the ratio of the number of events in the 81 keV photoelectron peak to that in the 356 keV photoelectron peak. The horizontal band is from the experimental data. The vertical band determines the dead layer thickness by comparing the experimental ratio and simulation fitting line. The error bars for the simulation points are smaller than the data point size and invisible in the plot.

Table 3. The estimated dead layer thicknesses with statistical uncertainties for different energy ratios of photoelectron peaks.

enegy peaks /81 keV	dead layer thickness /mm	stat. uncertainty /mm
276 keV	0.994	0.033
303 keV	1.035	0.025
356 keV	1.027	0.020
384 keV	1.010	0.032

Step 2: The statistical uncertainties of the energy peak ratios were added to the experimental result. The width of the blue band shown in Fig. 10 represents this statistical uncertainty. The blue band has two intersections with the black line. A red band was derived from the two intersections in Fig. 10: this is the statistical uncertainty of the dead layer thickness. All the statistical

uncertainties were obtained by this method and are also shown in Table 3.

Step 3: From all the results in Table 3, the central value and statistical uncertainty of the dead layer thickness was derived with the weighted average method and found to be 1.021 $\pm$0.013 mm.

4.3.2 Systematic uncertainties

The systematic uncertainties arise from:

(1) Event selections and rejections

The systematic uncertainty caused by event selection from the preamplifier reset period was derived in three steps. Firstly, the T_- cut was scanned from 0.18 s to 0.22 s. Secondly, by using the same method as T_-= 0.2 s, new results from the new T_- cut were obtained. Finally, by comparing the new results to the old result, the systematic uncertainty caused by event selection from preamplifier reset period was found to be 0.004 mm.

The systematic uncertainty caused by accidental coincidence event rejection was derived by changing the normal signal selection region from 3σ region to 5σ region, and found to be 0.003 mm.

(2) Accuracy of source location and detector dimensions

The systematic uncertainties related to the source location uncertainty of 1 mm, the endcap dimension uncertainty of 0.1 mm and the crystal dimension uncertainty of 0.1 mm were considered. For the endcap dimension uncertainty, which is the leading systematic uncertainty, another two new dead layer thickness were re-calculated by using the dimensions of 1.4 mm and 1.6 mm. The systematic uncertainty was obtained from the difference between the dead layer thickness of 1.5 mm endcap dimension and the two new dead layer thicknesses. The same method was applied to get the systematic uncertainties caused by accuracy of source positions, and the accuracy of crystal dimensions.

All the systematic uncertainties are listed in Table 4.

After all the uncertainties including statistical uncertainty and systematic uncertainties were considered, the dead layer thickness of the CDEX-1A PPCGe detector was derived to be 1.02$\pm$0.14 mm. Statistical and systematic uncertainties were studied in detail and the endcap dimension accuracy contributed more than 90% of the total systematic uncertainty. This result was also cross-checked by changing the ^{133}Ba source position from 73 mm to three other positions of 42 mm, 113 mm and 159 mm with measured values of 1.03 mm, 1.00 mm and 1.03 mm, respectively. A good agreement was derived among these different source positions.

Table 4. Systematic uncertainties.

event selection from preamplifier reset period	0.004 mm
accidental coincidence event rejection	0.003 mm
source location accuracy	0.005 mm
endcap dimension accuracy	0.135 mm
crystal dimension accuracy	0.022 mm
total systematic uncertainty	0.137 mm

5 Conclusion

This paper presents the procedure used for the measurement of the dead layer of the CDEX-1A detector. In this study, a ^{133}Ba source was used to measure the dead layer thickness. The crystal of this detector was fabricated with a side-hold structure made of OHFC and other material of which the depth is not uniform. We just measured the top dead layer and assume the lateral dead layer is the same. In our experiment, the dead layer thickness was measured to be 1.02 mm, which has a huge disagreement with the result of 0.5 mm given by the manufacturer. The dead layer thickness gives rise to a fiducial mass of 915 g with an uncertainty of 1.0%. This is the first time to measure and obtain the dead layer thickness of a PPCGe detector with ultra-low energy threshold of $\sim$400 eV, which is quite suitable to directly detect light dark matter. This result is important for the CDEX-1A experiment to calculate the fiducial mass of the PPCGe detector and further analyse the real data.

References

1 Q. Yue et al, Phys. Rev. D, **90**: 091701(R) (2014)
2 P. N. Luke et al, IEEE Trans. Nucl. Sci., **36**: 926–930 (1989)
3 W. Zhao et al, Phys. Rev. D, **88**: 052004 (2013)
4 Z. F. LV et al, Chinese Physics C, **36(9)**: 855–860 (2012)
5 C. E. Aalseth et al, Phys. Rev. Lett., **106**: 131301 (2011)
6 E. Aguayo et al, Nucl. Instrum. Methods A, **701**: 176–185 (2013)
7 J. L. Campbell et al, Nucl. Instrum. Methods, **117**: 519–532 (1974)
8 P. A. Burns et al, Nucl. Instrum. Methods A, **286**: 480–489 (1990)
9 A. Clouvas et al, Health Physics, **74**: 216–230 (1998)
10 N. Q. Huy et al, Nucl. Instrum. Methods A, **573**: 384–388 (2007)
11 YU. KHAZOV, A. RODIONOV, Nuclear Data Sheets, **112**: 935–936 (2011)
12 M. Agostini et al, Journal of Instrumentation, **6**: P04005 (2011)
13 S.K.Liu et al, Phys. Rev. D, **90**: 032003 (2014)
14 Glenn F. Knoll, *Radiation Detection and Measurement Fourth Edition* (Hoboken, New Jersey: John Wiley&Sons,2010), p. 691
15 J. Allison et al, IEEE Trans. Nucl. Sci., **53**(1): 270–278 (2006)
16 S. Agostinelli et al, Nucl. Instrum. Methods A, **506**: 250–303 (2003)
17 J. Su et al, Nucl. Instrum. Methods A, **763**: 364–371 (2014)